



## Automatic Chest CT Image Findings of Novel Coronavirus Pneumonia (COVID-19) Using U-Net Based Convolutional Neural Network

**S. Akila Agnes** 

Assistant Professor, Department of Computer Science and Engineering, Karunya Institute of Technology and Sciences, India. E-mail: akilaagnes@karunya.edu

**J. Anitha\***

\*Corresponding Author, Assistant Professor, Department of Computer Science and Engineering, Karunya Institute of Technology and Sciences, India. E-mail: anitha\_j@karunya.edu

**A. Arun Solomon** 

Assistant Professor, Department of Civil Engineering, Karunya Institute of Technology and Sciences, India. E-mail: arunsoloman@karunya.edu

---

### Abstract

The continuing outbreak of COVID-19 pneumonia is globally concerning. Timely detection of infection ensures prompt quarantine of patient which is crucial for preventing the rapid spread of this contagious disease and also supports the patient with necessary medication. Due to the high infection rate of COVID-19, our health management system needs an automatic diagnosis tool that equips the health workers to pay immediate attention to the needy person. Chest CT is an essential imaging technique for diagnosis and staging of 2019 novel coronavirus disease (COVID-19). The identification of COVID-19 CT findings assists health workers on further clinical evaluation, especially when the findings on CT scans are trivial, the person may be recommended for Reverse-transcription polymerase chain reaction (RT-PCR) tests. Literature reported that the ground-glass opacity (GGO) with or without consolidation are dominant CT findings in COVID-19 patients. In this paper, the U-Net based segmentation approach is proposed to automatically segment and analyze the GGO and consolidation findings in the chest CT scan. The performance of this system is evaluated by comparing the auto-segmented infection regions with the manually-outlines ones on 100 axial chests CT scans of around 40 COVID-19 patients from SIRM dataset. The proposed U-Net with pre-process approach yields specificity of  $0.91 \pm 0.09$  and sensitivity of  $0.87 \pm 0.07$  on segmenting GGO region and specificity of  $0.81 \pm 0.13$  and sensitivity of  $0.44 \pm 0.17$  on segmenting consolidation region. Also the

experimental results confirmed that the automatic detection method identifies the CT finding with a precise opacification percentage from the chest CT image.

**Keywords:** COVID-19, CT imaging findings, Segmentation, Deep learning, Ground-glass opacities, U-Net.

DOI: 10.22059/jitm.2020.79188

© University of Tehran, Faculty of Management

## Introduction

2019 novel coronavirus disease (COVID-19) is a communicable disease caused by severe acute respiratory syndrome coronavirus 2 (SARS-CoV-2), previously known as 2019 novel coronavirus (2019-nCoV). In December 2019, the first cases were reported in Wuhan, China, before spreading globally (Zhu et al., 2020) (Hui et al., 2020). The World Health Organization (WHO) declared a world health epidemic on January 30, 2020, further declared this as a pandemic on March 11, 2020 (Mahase, 2020). As on September 19th, in the first nine months of the outbreak, there have been 30,781,594 cases of COVID-19 across worldwide including 957,778 deaths, working out to a mortality rate of 3.11% (worldometers.info/: 19 September 2020). Many countries have been affected, and numerous cases of community spread are reported. In this epidemic situation, manual delineation of lung infection is a time-consuming and labor-intensive process. In that contact, health care workers need an automatic sensitive diagnostic tool to investigate potential COVID-19 cases.

RT-PCR or reverse transcription-polymerase chain reaction tool is commonly used for diagnosis of COVID-19. The study carried out by Fang et al. reported the issues with access to RT-PCR and the sensitivity of CT in identifying COVID-19 infection (Fang et al., 2020). In their study, they analyzed the reports of 51 confirmed COVID-19 patients and the CT scans acquired at different time intervals during their COVID-19 infection period. They found that 50 out of 51 patients (98%) had unusual findings from benchmark CT scans, but only 36 out of 51 patients (71%) had positive in the initial RT-PCR tests. Long et al. have made a comparative study on the sensitivity of both CT and rRT-PCR examination on COVID-19 pneumonia (Long et al., 2020). They concluded that the patients with typical CT findings and initial false-negative results with rRT-PCR can be quarantined, and also rRT-PCR test should be repeated to avoid misdiagnosis. Ai et al. have reported 97% sensitivity of CT in diagnosing COVID-19 and reported the limitations of RT-PCR (Ai et al., 2020).

Bernheim et al. have reported that the chest CT findings are normal at the earlier stage of COVID-19 and change gradually from small lobular to irregular patchy GGOs as the disease progresses (Bernheim et al., 2020). Kanne et al. have stated that the general diagnostic CT findings of COVID-19 pneumonia, which includes bilateral, peripheral or rounded

ground-glass opacities with or without consolidation (Kanne, 2020). Meng et.al have concluded that CT scan has huge importance in identifying patients with COVID-19 pneumonia, particularly in the highly suspicious cases with negative lab test results (Meng et al., 2020).

As stated by the current diagnostic criteria (Commission & others, 2020), etiological examinations (such as swab tests) have emerged as the gold standard for examining SARS-CoV-2 infection. The time-consuming laboratory test procedures may delay the patient isolation process and increase the transmission of infection. Also, the sensitivity of these laboratory tests could not meet the demands of the increasing infected population. Hence most of the literature stated that the sensitivity of CT scan is higher than rRT-PCR tests, therefore the Chest CT screening is recommended for patients with COVID-19-compatible clinical and epidemiological features. As the chest CT has a high sensitivity for the screening of COVID-19, this may be considered as an important tool for the current detection of COVID-19 in epidemic areas (Ai et al., 2020). When patients have clinical signs, epidemiological characteristics, and chest CT imaging characteristics of COVID-19 pneumonia, will be considered for quarantine and treatment (Hao & Li, 2020).

The worst-case scenario of COVID-19 is the high rate of infection, so more number of people gets infected at the same time. On this epidemic scenario, our health management system needs an automatic diagnosis tool to identify the disease quickly and reduce the spread out by isolating the infected person immediately. The chest CT findings may consider for patient initial isolation, but then the patient gets through confirmatory testing and appropriate treatment. Radiology literature confirmed that the Ground glass opacity is usually the first sign of COVID-19 and is followed by consolidation.

Recent studies (Ye et al. 2020) have shown evidence of infection, such as early-stage ground-glass opacity (GGO) and late-stage white consolidation observed from CT images. Therefore, a qualitative assessment of the infection could provide useful information for the treatment of COVID-19 infections. The objective of this work is to develop an automatic tool for segmenting the lung infections from CT scan with high sensitivity. In recent years, Deep learning (DL) has obtained remarkable results in various medical imaging processes such as segmentation and classification. The principal advance of deep learning approach is the end-to-end learning behavior, which finds the solution without the domain expertise. This cutting-edge feature brings many researchers of medical image analysis towards DL approach. The popular DL based segmentation models such as a fully convolutional neural network (FCN) (Shelhamer, Long, & Darrell, 2017), Deep encoder and decoder model for image segmentation (Badrinarayanan, Kendall, & Cipolla, 2017), and U-Net convolutional network for medical image segmentation (Ronneberger, Fischer, & Brox, 2015) have been utilised in various medical image segmentation applications. Khagi et.al, have suggested that the SegNet

with certain alterations, can be used in medical MRI image segmentation (Khagi & Kwon, 2018). All these convolutional neural networks (CNN) based semantic segmentation models have symmetrical architecture consists of an encoder and an equivalent decoder structures. The segmentation model acquires the abstract level spatial and contextual details from the annotated datasets and learns to predict the segmentation map.

U-Net is an improved CNN that is designed to segment exclusively medical images. It is widely employed on a range of medical image analysis tasks such as liver segmentation and breast segmentation. Hybrid densely connected UNet (H-DenseUNet)(Li et al., 2018), which consists of a 2-D DenseUNet for segmenting liver tumor efficiently. Zhou et.al (Zhou, Siddiquee, Tajbakhsh, & Liang, 2018) have proposed nested U-Net Architecture (UNet++) for medical image segmentation tasks such as nuclei segmentation in the microscopy images, liver segmentation in abdominal CT scans, nodule segmentation in chest CT scans, and polyp segmentation in colonoscopy videos. They concluded that UNet++architecture achieves improved performance than standard UNet. Agnes et.al (Agnes, Anitha, & Peter, 2018) have proposed a U-Net based Convolutional Deep and Wide network (CDWN) model to separate the lungs from chest CT scans accurately without any post-processing operations. U-Net produces promising results in the medical image analysis domain. In this paper a U-Net based approach is proposed to segment and quantify the common CT findings of COVID-19 (GGO + Consolidation).

The remainder of the paper is structured as follows. Next section discusses the methodology used to build the U-Net model for GGO segmentation and chest CT consolidation regions. The Outcome and Discussion section presents and discusses the quantitative and qualitative evaluation of the proposed work. The conclusion is given in the last section.

## Materials and Methods

### Dataset

The proposed work has examined on COVID-19 CT segmentation dataset prepared by the Italian Society of Medical Radiology and Interventional (SIRM), which consists of 100 axial CT images taken from >40 patients with COVID-19. The CT images have been resized into 512x512 pixels and saved in NII (or NIfTI) format. The pixel values are given in Hounsfield units. The images have been contoured manually by a radiologist into 3 labels, which involves ground-glass opacity (GGO), consolidation (C), and pleural effusion. This work is focused on segmenting the most common CT image findings of COVID-19 such as ground-glass opacity and consolidation from CT scan. Figure 1 depicts the sample image considered for training the U-Net model.

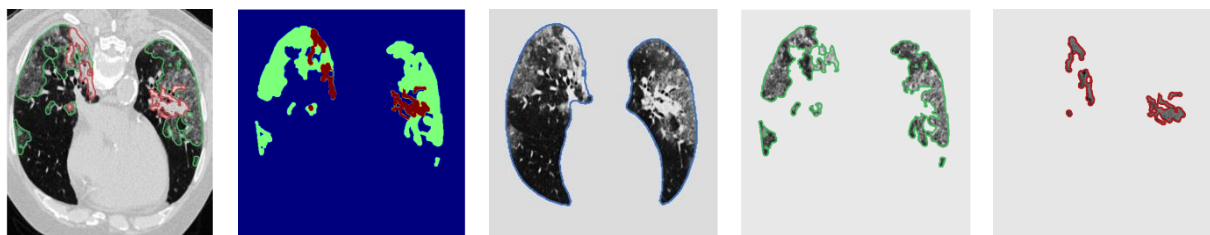


**Figure 1.** Sample image (SIRM Case 31 - Slice position: 75, Patient Age: 63, Gender: Male) from SIRM dataset and its various segments. Column (from left to right) (1) Original CT image (ground-glass opacity: green, consolidation: red) (2) Manual segmented mask (ground-glass opacity: green, consolidation: red) (3) Segmented lungs (4) Ground-glass opacity region (5) Consolidation region.

### COVID-19 Chest CT Imaging Features

Chest CT scan can be considered as an initial examination at the health care center for admitting the suspected people and further, the disease can be confirmed via the main diagnostic tools of COVID-19. Sample axial CT image of confirmed COVID-19 patient with ground-glass opacities and solid consolidation is shown in Figure 2. Ground-glass opacification are tiny air pouches or alveoli that are filled with fluid and turn the shade of gray on a CT scan. Throughout the advanced stage of infection, more and more fluid will collect in the lung lobes, so that the appearance of ground glass will move to a solid when being accumulated. These CT findings are seen either in isolation or in combination. These abnormalities commonly happen in multiple lobes, and more frequently affect the edge of the lungs. A histogram is plotted from 50 arbitrary axial slices of CT scans of COVID-19 cases from the SIRM training set to demonstrate the Hounsfield units (HU) distribution of various regions in chest CT scan images and shown in Figure 3.

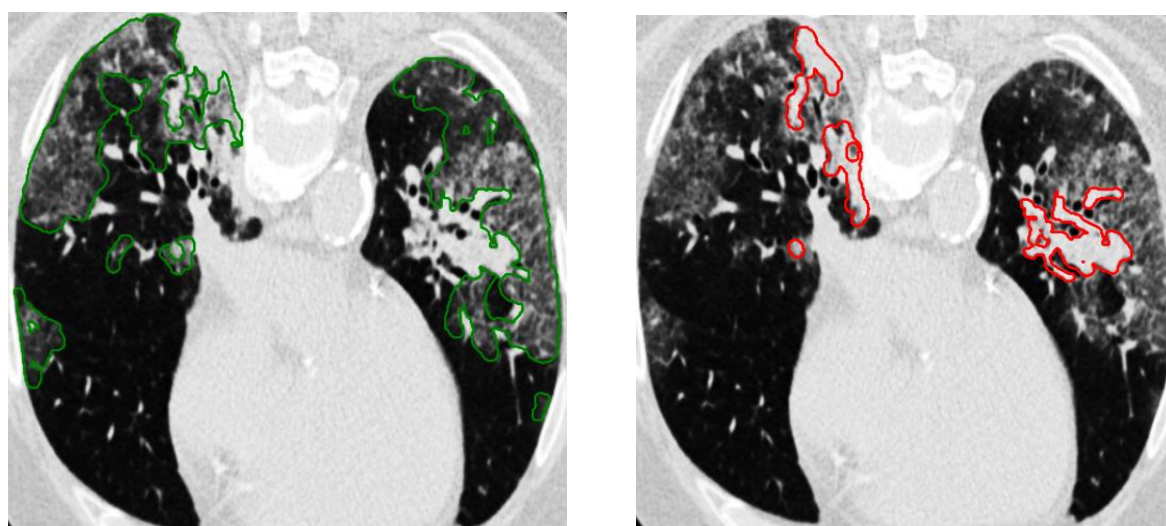


**Figure2.** Sample axial CT image of confirmed COVID-19 patient from SIRM dataset with ground-glass opacities with solid consolidation scattered throughout the lungs. From left to right: (1) ground-glass opacities (green border) (2) consolidation (red border).

The histogram plot shows that the infected region falls on the right tail of lung region distribution. This confirms that the infected region has higher HU value than the normal lung region pixels. The HU distribution of consolidation region is present on the right side of GGO regions; this indicates that the intensity of consolidation region is higher than the GGO region. As the ranges of the lungs, GGO and consolidation regions are overlapped; a simple thresholding technique might not be suitable for separating the regions. Therefore complex features or algorithms are required to segment the regions accurately.

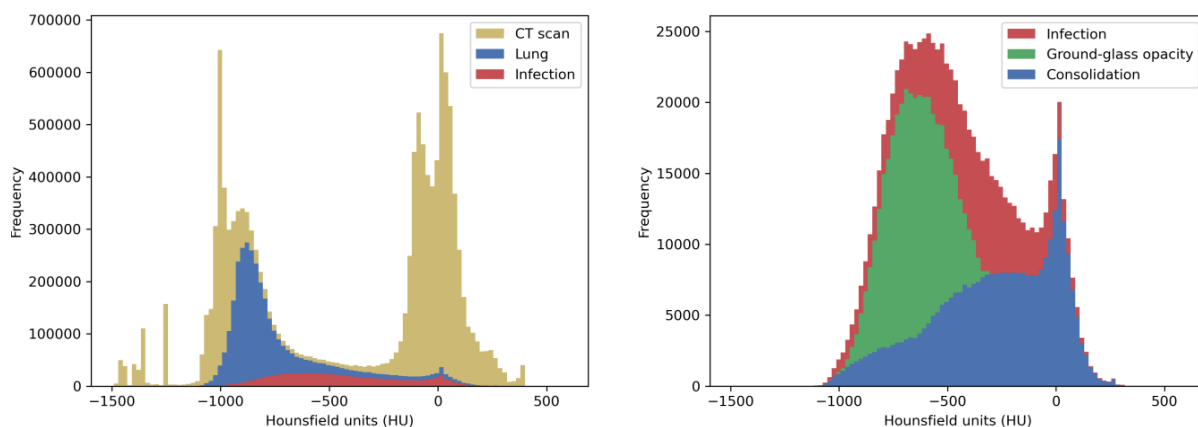


**Figure 3. HU value histogram of 50 arbitrary axial slices of CT scans of COVID-19 cases from the SIRM training set: HU distribution of the lungs and infection in the whole CT image (left) and HU distribution of GGO and consolidation in the infected region (right).**

### U-Net model

The U-Net model for lung infection segmentation performs an overall pixel-wise categorization on chest CT scan in a supervised manner. U-Net is a popular model used for medical image segmentation because the model can be built with few training samples. It consists of an encoder followed by the symmetrical decoder and ended by soft-max segmentation layer. The encoder part consists of an ordered set of convolutional, batch normalization, max-pooling and drop out layers. The convolutional layers in the U-Net can be interpreted as feature extractor and the max-pooling layers can be interpreted as feature reducer. And the decoder part does the learnable up-sampling operation through the transpose convolutional layer. The transpose convolution layer expands the feature map computed by the encoder with the learnable kernels. Apart from the sequential connections, the decoder part of the U-Net model has a special inter-block connection between encoder side convolutional and decoder side de-convolutional layers. This helps the network to learn vital information by combining the same dimension feature map generated by the decoder and the corresponding encoder block. At the final layer, the Softmax activation function triggers every pixel in the feature map and produces a probability map which is transferred to a segmentation mask.

In this work, GGO and consolidation parts are segmented from the CT scan image in two methods. In the first method, the raw CT scan is given as input for the U-Net model to segment the infected regions. This approach does not require any pre-processing steps. The second approach needs pre-processing technique to separate the lung parenchyma from the CT image and then the segmented image will be given as input to the U-Net model for segmenting the infected parts. For this experiment, the lung regions are segmented from the input chest CT scan images using the existing convolutional deep and wide network (CDWN) model (Agnes et al., 2018). The segmentation of lungs removes unwanted data from the CT image that enables the U-Net model to locate the infection regions in the lungs faster and better.

### **Training Configuration of U-Net Model**

The summary of the U-Net model implemented in this experiment is presented in Table 1. The encoding portion of the implemented U-Net includes four sets of convolutional and max-pooling layers, generating a collection of feature maps from the image data. The convolutional layer performs convolution operation on the padded image with 3x3 kernel and stride of 2. Max-pooling layer compresses the feature map by pooling the maximum value in the window size of 2x2. Dropout layer is added between convolutional layers to improve the network performance. The decoder path converts low dimension feature map to high dimension feature map through a sequence of trainable de-convolutional layers (Transposed convolution). The transposed convolution operation does upsample with 3x3 kernel and stride of 2. As the model is segmenting two regions (GGO and consolidation) from the chest CT scan, the final segmentation layer generates three categorized images (GGO, consolidation, and other) with the same dimension of the input image.

During the phase of training, the U-Net model is prepared with a set of annotated CT images. The network training starts with the random weight and kernel values. The image data is mapped into a categorical image through a series of convolution and de-convolution operations. The model has set dynamic learning rate (LR) starting with 0.00001 and defined batch size of 10. When the performance of the model has stopped improving, the learning rate is reduced by a factor 0.1 (new LR = LR \* factor). Adam optimizer is used for compiling the model and binary cross-entropy loss function is used as a cost function to find the optimal set of kernels and weights for the model. For smooth segmentation a constant kernel size of 3x3 is set in all convolutional and de-convolution layers (Agnes et al., 2018). All convolutional and de-convolutional layers used ReLU activation function due to its fast computation during the training phase. Dropout with a rate of 0.5 is applied between all connected layers to avoid network overfitting. The U-Net model is implemented with TensorFlow2.0 and Keras in python.

**Table 1. U-Net model summary**

| Layer        | Type            | Input shape      | Connected to          | Output shape  |
|--------------|-----------------|------------------|-----------------------|---------------|
| Image        | Input           | 512X 512X 1      | N/A                   | 512X 512X 1   |
| conv1        | Convolution2D   | 512X 512X 1      | Image                 | 512X 512X 16  |
| pool1        | MaxPooling2D    | 512X 512X 16     | conv1                 | 256X 256X 16  |
| conv2        | Convolution2D   | 256X 256X 16     | pool1                 | 256X 256X 32  |
| pool2        | MaxPooling2D    | 256X 256X 32     | conv2                 | 128X 128X 32  |
| conv3        | Convolution2D   | 128X 128X 32     | pool2                 | 128X 128X 64  |
| pool3        | MaxPooling2D    | 128X 128X 34     | conv3                 | 64X 64X 64    |
| conv4        | Convolution2D   | 64X 64X 64       | pool3                 | 64X 64X 128   |
| pool4        | MaxPooling2D    | 64X 64X 66       | conv4                 | 32X 32X 128   |
| conv5        | Convolution2D   | 32X 32X 128      | pool4                 | 32X 32X 256   |
| convtrans1   | Conv2DTranspose | 32X 32X 130      | conv5                 | 64X 64X 128   |
| concatenate1 | Concatenate     | 2 @ 64X 64X 128  | convtrans1 ,<br>conv4 | 64X 64X 256   |
| conv6        | Convolution2D   | 64X 64X 256      | concatenate1          | 64X 64X 128   |
| convtrans2   | Conv2DTranspose | 64X 64X 128      | conv6                 | 128X 128X 64  |
| concatenate2 | Concatenate     | 2 @ 128X 128X 64 | convtrans2,<br>conv3  | 128X 128X 128 |
| conv7        | Convolution2D   | 128X 128X 128    | concatenate2          | 128X 128X 64  |
| convtrans3   | Conv2DTranspose | 128X 128X 64     | conv7                 | 256X 256X 32  |
| concatenate3 | Concatenate     | 2 @ 256X 256X 32 | convtrans3 ,<br>conv2 | 256X 256X 64  |
| conv8        | Convolution2D   | 256X 256X 64     | concatenate3          | 256X 256X 32  |
| convtrans4   | Conv2DTranspose | 256X 256X 32     | conv8                 | 512X 512X 16  |
| concatenate4 | Concatenate     | 2 @ 512X 512X 16 | convtrans4,<br>conv1  | 512X 512X 32  |
| conv9        | Convolution2D   | 512X 512X 32     | concatenate4          | 512X 512X 16  |
| conv10       | Convolution2D   | 512X 512X 16     | conv9                 | 512X 512X 3   |

## Results and discussions

The segmentation results are quantitatively assessed with dice coefficient, Hausdorff distance (HD), accuracy, specificity, sensitivity and f1-score. The dice coefficient calculates the spatial overlay between the segmentation result and the manual segmentation result. In the dice coefficient measure, a value of one indicates the perfect spatial intersection between the ground truth result and zero represents no spatial overlap. Hausdorff distance measures the similarity by considering the boundary of two segmented regions. The smaller HD value indicates the best match. In medical image segmentation, the term True Positive denotes the

correct prediction rate of positive pixels, True Negative denotes correct prediction rate of negative pixels, False Positive indicates the wrong prediction rate of negative pixels and False Negative denotes the wrong prediction rate of positive pixels. The sensitivity reflects the ratio of true positives to the number of true and false negatives. The specificity reflects the ratio of true negatives to the number of true negatives and false positives. The segmentation model is said to be perfect when the accuracy, specificity, sensitivity values between ground truth result and the segmented result are closer to one. F1-score is computed by dividing the number of correct positive results by the number of all positive results returned by the model. F1-score gives the harmonic mean of sensitivity and specificity; the perfect segmentation F1-score value is one.

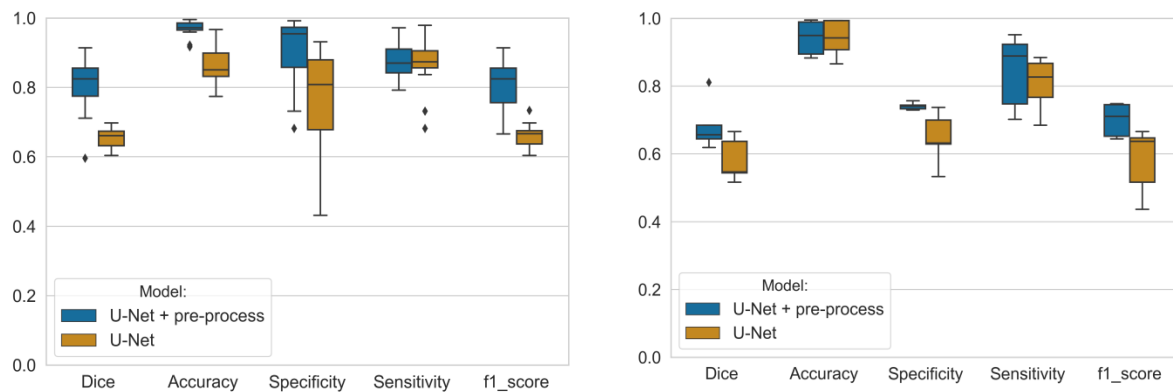


**Figure 4. Box plot of U-Net Performance on segmenting infected lung areas. (left) ground glass opacity and (right) consolidation. The middle line of the box shows the median in the figure, the boxes are extended to the lower and upper quartiles, the whiskers are the most extreme values, and the diamonds denotes the outliers.**

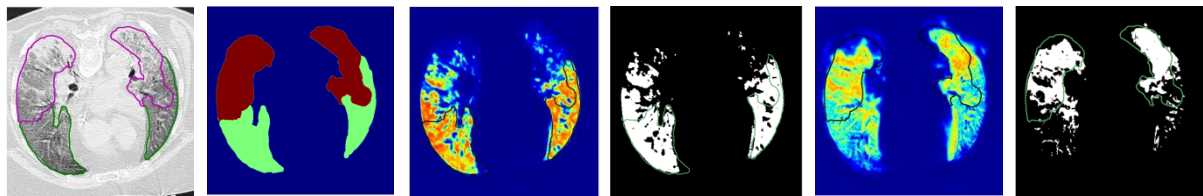
The statistical summaries of segmentation results produced by U-Net with and without pre-process approaches are presented with boxplot graph in Figure 4. The box plot shows the distribution of segmentation results of the two U-Net based segmentation approaches on the validation set. Both approaches provide consistent results with the manual segmentation in terms of dice coefficient, Hausdorff distance, accuracy, sensitivity, and f1-score. But the specificity of the U-Net + pre-process approach in segmenting GGO region is distributed in the range of 0.68 – 0.99 and consolidation region is distributed in the range of 0.51-0.93. This shows that the model could predict positive pixels accurately but not able to predict the negative pixels precisely.

Table 2 summarizes the segmentation scores obtained by U-Net with and without pre-process on SIRM dataset. The attained results demonstrate that the U-Net with pre-process approach achieves 15%, 14%, 1% and 40% improvement on segmenting GGO region over U-Net without pre-processing in terms of dice coefficient, Hausdorff distance, accuracy, and specificity respectively. Similarly, the U-Net with pre-processing approach achieves 23%,

7%, 15%, and 3% improvement on segmenting consolidation region over U-Net without pre-processing in terms of dice coefficient, Hausdorff distance, accuracy, and specificity respectively. In summary, the U-Net + pre-process segment the CT findings GGO and consolidation regions with improved dice coefficient, Hausdorff distance, accuracy and specificity.

**Table 2. Evaluation results of U-Net with and without pre-processing on SIRM Dataset**

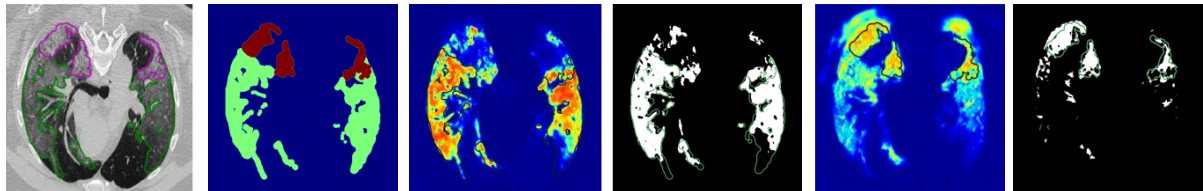
| Classes              | Methods             | Dice      | Hausdorff | Accuracy  | Specificity | Sensitivity |
|----------------------|---------------------|-----------|-----------|-----------|-------------|-------------|
| Ground-glass opacity | U-Net               | 0.69±0.06 | 8.61±2.46 | 0.96±0.03 | 0.91±0.09   | 0.62±0.11   |
|                      | U-Net + pre-process | 0.80±0.09 | 7.55±1.71 | 0.97±0.02 | 0.91±0.09   | 0.87±0.07   |
| Consolidation        | U-Net               | 0.55±0.1  | 8.92±3.33 | 0.94±0.06 | 0.64±0.17   | 0.81±0.13   |
|                      | U-Net + pre-process | 0.68±0.08 | 9.62±3.25 | 0.94±0.05 | 0.74±0.01   | 0.84±0.11   |



**SIRM Case 5** - Slice position:88, Patient Age:64, Gender:Male

**Manual Diagnosis** - Opacification percentage of the lung: 88.2%

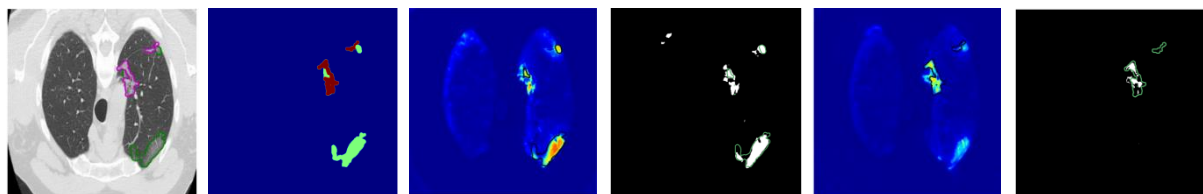
**Prediction** - Opacification percentage of the lung: 113.9%



**SIRM Case 28** - Slice position:64, Patient Age:48, Gender:Female

**Manual Diagnosis** - Opacification percentage of the lung: 50.3%

**Prediction** - Opacification percentage of the lung: 59.2%



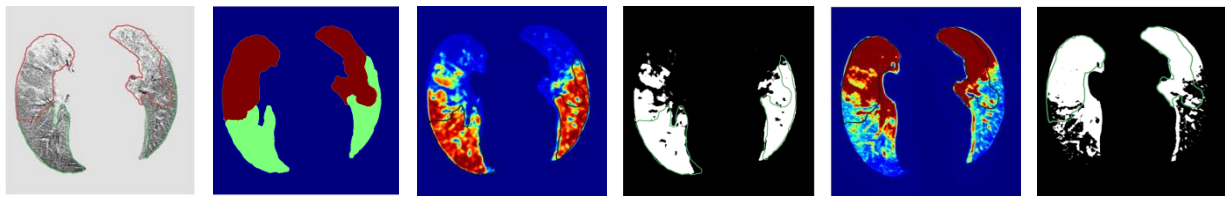
**SIRM Case 47** - Slice position:51, Patient Age:61, Gender:Male

**Manual Diagnosis** - Opacification percentage of the lung: 8.1%

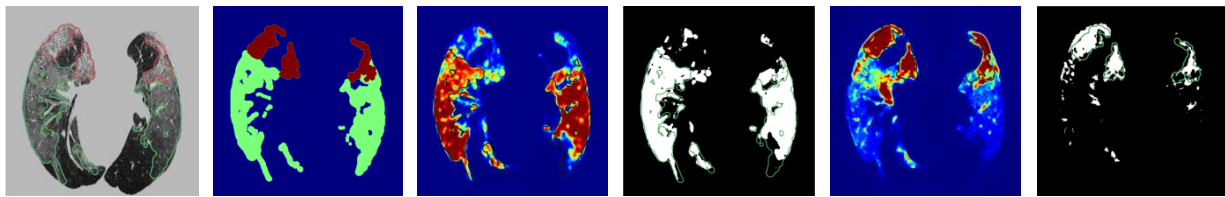
**Prediction** - Opacification percentage of the lung: 6.7%

**Figure 5. Example of CT findings segmentation results of U-Net Model. Column (from left to right) (1) CT image (2) Manual ground truth (GGO: red, C: green) (3) Predicted probability matrix represents GGO (manual segmentation: black border) (4) Segmented GGO mask (manual segmentation: green) (5) Predicted probability matrix represents Consolidation (manual segmentation: black) (6) Segmented Consolidation mask: (manual segmentation: green)**

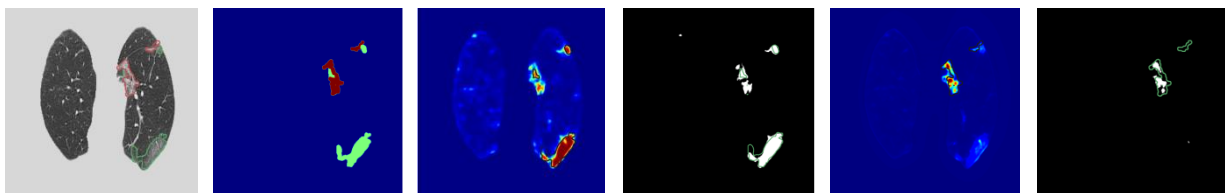
The sample visual segmentation results of U-Net without pre-processing are shown in Figure 5 and U-Net with pre-processing is shown in Figure 6. The sample CT images of COVID-19 confirmed cases that contain both GGO and consolidation findings are taken for visual comparison. As well the selected images showing the best (SIRM Case 47) and worst (SIRM Case 5) case segmentation results. The contours of ground truth results are highlighted with green borders to compare with the predicted results. The obtained results show that the contours delineated by both U-Net models are matched well with the manual segmentation boundaries except SIRM Case 5.



SIRM Case 5 - Slice position:88, Patient Age:64, Gender:Male  
 Manual Diagnosis - Opacification percentage of the lung: 88.2%  
 Prediction - Opacification percentage of the lung: 85.3%



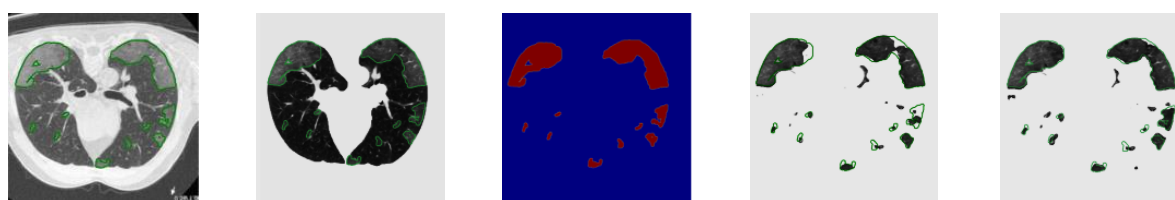
SIRM Case 28 - Slice position:64, Patient Age:48, Gender:Female  
 Manual Diagnosis - Opacification percentage of the lung: 50.3%  
 Prediction - Opacification percentage of the lung: 48.5%



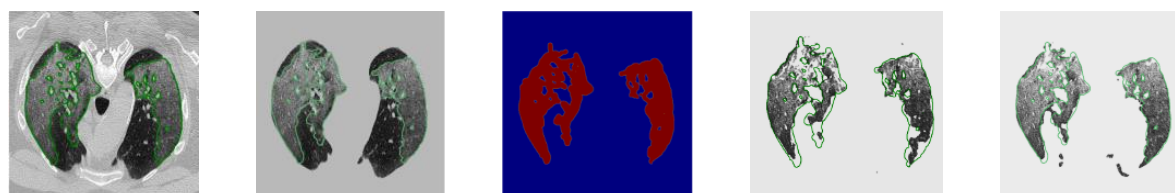
SIRM Case 47 - Slice position:51, Patient Age:61, Gender:Male  
 Manual Diagnosis - Opacification percentage of the lung: 8.1%,  
 Prediction - Opacification percentage of the lung: 7.2%,

**Figure 6. Example of CT findings segmentation results of U-Net + pre-process approach. Column (from left to right) (1) pre-processed CT image (2) Manual segmentation (GG: red, C: green) (3) Predicted probability matrix represents GGO (manual segmentation: black) (4) Segmented GGO mask: red (manual segmentation: green) (5) Predicted probability matrix represents Consolidation (manual segmentation: black) (4) Segmented Consolidation mask: red (manual segmentation: magenta)**

Figure 7 shows the sample segmented GGO regions from the chest CT scan image. When comparing the segmented GGO regions obtained by the two approaches, it is obvious that the U-Net + Pre-process approach could segment the regions with more sensitivity. As well the predicted region edges of U-Net + pre-process is exactly matched with the manual segmentation edges.



SIRM Case 28 - Slice position: 61, Patient Age: 48, Gender: Female



SIRM Case 47 - Slice position: 96, Patient Age: 61, Gender: Male

**Figure 7. Example segmented CT findings from U-Net and U-Net + pre-process approaches. Column (from left to right) (1) CT image (2) Segmentation Lungs (GGO: green) (3) GGO mask (4) Predicted GGO region from whole CT image (manual segmentation: green) (5) Predicted GGO region from segmented lungs (manual segmentation: green)**

Table 3 presents the actual and predicted opacification percentage of few samples confirmed COVID-19 cases. Quantitative opacification analysis helps to determine the degrees of clinical severity. Also helps to investigate the progression of the disease severity. The segmented CT findings are compared with ground truth findings in terms of opacification percentage. From Table 3, it is observed that the predicted opacification rate (GGO + consolidation) of proposed U-Net + pre-process approach is close to the actual opacification rate rather than U-Net without pre-processing.

**Table 3. Comparison of actual and predicted opacification percentage**

| Case no – Slice no | Actual opacification % of the Lung | Predicted opacification % of the lung |                     |
|--------------------|------------------------------------|---------------------------------------|---------------------|
|                    |                                    | U-Net                                 | U-Net + pre-process |
| SIRM 05-88         | 88.2%                              | 100%                                  | 85.3%               |
| SIRM 14-80         | 5.17%                              | 7.6%                                  | 6.9%                |
| SIRM 28-61         | 24.1%                              | 22.8%                                 | 23.4%               |
| SIRM 28-64         | 50.3%                              | 59.2%                                 | 48.5%               |
| SIRM 47-51         | 8.1%                               | 6.7%                                  | 7.2%                |
| SIRM 47-96         | 55.6%                              | 71.1%                                 | 58.1%               |

In summary, the proposed U-Net + pre-process approach could detect the common CT findings of COVID-19 pneumonia with decent specificity of  $0.91 \pm 0.09$  (GGO) and  $0.74 \pm 0.01$  (consolidation) and sensitivity of  $0.87 \pm 0.07$  (GGO) and  $0.84 \pm 0.11$  (consolidation). Both quantitative and visual analysis of the segmented results confirms that the U-Net + pre-

process approach provides accurate results for quantitative assessment of COVID-19 infection in CT scans. Also, the U-Net + pre-process approach has accurately predicted the opacification percentage (GGO + consolidation) close to the actual opacification percentage.

## Conclusion

The automatic delineation of infected lung regions is a key component of COVID-19 diagnosis. Identification of CT findings of COVID-19 provides timely diagnostic evidence of the disease and enables early diagnosis and treatment. Also, the quantitative opacification analysis from CT images is an important procedure in of COVID-19 pneumonia treatment. So the automatic detection of CT image findings of novel coronavirus pneumonia (COVID-19) equips the health workers in diagnosing and assessing the severity of COVID-19 pneumonia. Deep learning based U-Net + pre-process approach has been implemented to locate and quantify the CT findings from the chest CT scan accurately. The experimental result concludes that the proposed U-Net + pre-process approach locates the CT findings with the specificity of  $0.91\pm 0.09$  (GGO) and  $0.74\pm 0.01$  (consolidation) and sensitivity of  $0.87\pm 0.07$  (GGO) and  $0.84\pm 0.11$  (consolidation). Therefore it is recommended to build the U-Net model with pre-processed CT image to gain improved segmentation performance on COVID-19 pneumonia diagnosis. This automated detection tool can be used for identifying the CT finding with an accurate opacification percentage. In future, this work can be extended to quantify the opacification.

## Acknowledgements

We thank the MedSeg for providing convenient download link of these 100 axial CT images from confirmed COVID-19 CT cases (<http://medicalsegmentation.com/covid19/>).

## References

- Agnes, S. A., Anitha, J., & Peter, J. D. (2018). Automatic lung segmentation in low-dose chest CT scans using convolutional deep and wide network (CDWN). *Neural Computing and Applications*, 1–11.
- Ai, T., Yang, Z., Hou, H., Zhan, C., Chen, C., Lv, Wenzhi., Qian., Xia & Liming. (2020). Correlation of chest CT and RT-PCR testing in coronavirus disease 2019 (COVID-19) in China: a report of 1014 cases. *Radiology*, 200642.
- Badrinarayanan, V., Kendall, A., & Cipolla, R. (2017). Segnet: A deep convolutional encoder-decoder architecture for image segmentation. *IEEE Transactions on Pattern Analysis and Machine Intelligence*, 39(12), 2481–2495.
- Bernheim, A., Mei, X., Huang, M., Yang, Y., Fayad, Z. A., Zhang, N. (2020). Chest CT findings in coronavirus disease-19 (COVID-19): relationship to duration of infection. *Radiology*, 200463.
- Commission, C. N. H., (2020). Diagnosis and treatment of pneumonitis caused by new coronavirus (trial version 6). *Beijing: China National Health Commission*.

- Fang, Y., Zhang, H., Xie, J., Lin, M., Ying, L., Pang, P., & Ji, W. (2020). Sensitivity of chest CT for COVID-19: comparison to RT-PCR. *Radiology*, 200432.
- Hao, W., & Li, M. (2020). Clinical diagnostic value of CT imaging in COVID-19 with multiple negative RT-PCR testing. *Travel Medicine and Infectious Disease*.
- Hui, D. S., Azhar, E. I., Madani, T. A., Ntoumi, F., Kock, R., Dar, O. (2020). The continuing 2019-nCoV epidemic threat of novel coronaviruses to global health—The latest 2019 novel coronavirus outbreak in Wuhan, China. *International Journal of Infectious Diseases*, 91, 264.
- Kanne, J. P. (2020). *Chest CT findings in 2019 novel coronavirus (2019-nCoV) infections from Wuhan, China: key points for the radiologist*. Radiological Society of North America.
- Khagi, B., & Kwon, G.-R. (2018). Pixel-Label-Based Segmentation of Cross-Sectional Brain MRI Using Simplified SegNet Architecture-Based CNN. *Journal of Healthcare Engineering*, 2018.
- Li, X., Chen, H., Qi, X., Dou, Q., Fu, C.-W., & Heng, P.-A. (2018). H-DenseUNet: hybrid densely connected UNet for liver and tumor segmentation from CT volumes. *IEEE Transactions on Medical Imaging*, 37(12), 2663–2674.
- Long, C., Xu, H., Shen, Q., Zhang, X., Fan, B., Wang, C., Li, H. (2020). Diagnosis of the Coronavirus disease (COVID-19): rRT-PCR or CT? *European Journal of Radiology*, 108961.
- Mahase, E. (2020). China coronavirus: WHO declares international emergency as death toll exceeds 200. *Bmj*, 368, m408.
- Meng, H., Xiong, R., He, R., Lin, W., Hao, B., Zhang, L. (2020). CT imaging and clinical course of asymptomatic cases with COVID-19 pneumonia at admission in Wuhan, China. *Journal of Infection*.
- Ronneberger, O., Fischer, P., & Brox, T. (2015). U-net: Convolutional networks for biomedical image segmentation. *International Conference on Medical Image Computing and Computer-Assisted Intervention*, 234–241.
- Shelhamer, E., Long, J., & Darrell, T. (2017). Fully convolutional networks for semantic segmentation. *IEEE Annals of the History of Computing*, (04), 640–651.
- Ye, Zheng et al. 2020. “Chest CT Manifestations of New Coronavirus Disease 2019 (COVID-19): A Pictorial Review.” *European radiology*: 1–9.
- Zhou, Z., Siddiquee, M. M. R., Tajbakhsh, N., & Liang, J. (2018). Unet++: A nested u-net architecture for medical image segmentation. In *Deep Learning in Medical Image Analysis and Multimodal Learning for Clinical Decision Support* (pp. 3–11). Springer.
- Zhu, N., Zhang, D., Wang, W., Li, X., Yang, B., Song, J. (2020). A novel coronavirus from patients with pneumonia in China, 2019. *New England Journal of Medicine*.

---

#### **Bibliographic information of this paper for citing:**

Akila Agnes, S., Anitha, J., & Arun Solomon, A. (2020). Automatic Chest CT Image Findings of Novel Coronavirus Pneumonia (COVID-19) Using U-Net Based Convolutional Neural Network. *Journal of Information Technology Management, Special Issue*, 22-35.